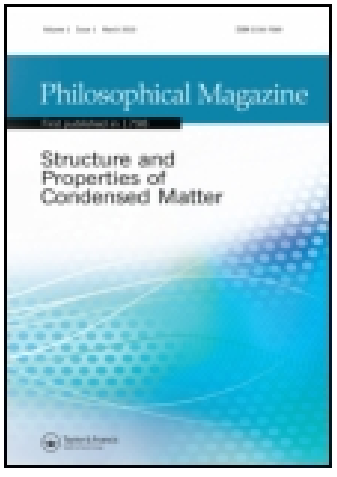

Philosophical Magazine
Publication details, including instructions for authors and subscription information:
http://www.tandfonline.com/loi/tphm20

Enhancing the performance of thin film CdS/PbS photovoltaic solar cells

H.A. Mohamed[ab]

[a] Faculty of Science, Physics Department, Sohag University, 82524 Sohag, Egypt

[b] Physics Department, Teachers College, King Saud University, 11148 Riyadh, Kingdom of Saudi Arabia

Published online: 25 Sep 2014.

To cite this article: H.A. Mohamed (2014) Enhancing the performance of thin film CdS/PbS photovoltaic solar cells, Philosophical Magazine, 94:30, 3467-3486, DOI: 10.1080/14786435.2014.961586

To link to this article: http://dx.doi.org/10.1080/14786435.2014.961586

Philosophical Magazine, 2014
Vol. 94, No. 30, 3467–3486, http://dx.doi.org/10.1080/14786435.2014.961586

Enhancing the performance of thin film CdS/PbS photovoltaic solar cells

H.A. Mohamed[a,b]*

[a]*Faculty of Science, Physics Department, Sohag University, 82524 Sohag, Egypt;* [b]*Physics Department, Teachers College, King Saud University, 11148 Riyadh, Kingdom of Saudi Arabia*

(*Received 8 April 2014; accepted 26 August 2014*)

This work investigates dependence of the short-circuit current density, open-circuit voltage, fill factor and efficiency of a thin film CdS/PbS solar cell on thickness of transparent conductive oxide (TCO) layer, thickness of window layer (CdS), concentration of uncompensated acceptors (width of space-charge region), carrier lifetime in PbS and the reflectivity from metallic back contact. The effect of optical losses, front and rear recombination losses as well as the recombination losses on space-charge region are also considered in this study. As a result, by thinning the front contact layer indium tin oxide from 400 to 100 nm and window layer (CdS) from 200 to 100 nm it is possible to reduce the optical losses from 32 to 20%. The effect of electron lifetime on the internal and external quantum efficiency can be neglected at high width of the space-charge region. The maximum current density of 18.4 mA/cm^2 is achieved at wide space-charge region (concentration of uncompensated acceptors = 10^{15} cm^{-3}) and the longest lifetime ($\tau_n = 10^{-6}$ s) where the optical and recombination losses are about 55%. The maximum efficiency of 5.17%, maximum open-circuit voltage of 417 mV and approximately fixed fill factor of 74% are yielded at optimum conditions such as: electron lifetime = 10^{-6} s; concentration of uncompensated acceptors = 10^{16} cm^{-3}; thickness of TCO = 100 nm; thickness of CdS = 100 nm; velocity of surface and rear recombination = 10^7 cm/s and thickness of absorber layer = 3 μm. When the reflectance from the back contact is 100%, the cell parameters improve and the cell efficiency records a value of 6.1% under the above conditions.

Keywords: CdS/PbS thin film solar cell; optical losses; recombination losses; open-circuit voltage; cell efficiency

1. Introduction

At present, photovoltaic solar cells are one of the most important renewable energy sources [1–3]. Most modern solar cells are made from either crystalline silicon or thin-film semiconductor material. Silicon cells are more efficient at converting sunlight to electricity, but generally have higher manufacturing costs [4]. Thin-film materials typically have lower efficiencies, but can be simpler and less costly to manufacture. The best efficiency results reported for three of the more relevant thin-film solar cell technologies are 18.3, 20 and 12.3% for CdS/CdTe, CdS/CIGS and a-Si, respectively [5].

*Email: hussein_abdelhafez2000@yahoo.com

The later types of solar cells have been fabricated on the basses of mid-range band-gap semiconductors which absorb in the visible range of the solar spectrum. Recently [6], materials with narrow optical energy gap such as lead sulphide (PbS), which has direct and narrow optical energy gap of 0.41 eV at 300 K, have been used as an absorber layer in thin film heterostructure solar cells. Although the choice of lead sulphide as an active absorbing layer in a solar cell can be considered unusual as the expected efficiency would be lower than what is actually attained in more conventional CdTe/CdS or CIGS/CdS solar cells, the recent advancements in this type of solar cells [7–10] have shown the convenience of developing solar cells based on PbS. The advantages of this type of solar cells are due to the unique properties of PbS, which can be summarized as follows: (1) PbS can absorb solar radiation near the infrared region of the solar spectrum, which is not absorbed by commonly used PV materials, (2) bulk-like PbS can be deposited by cheap, simple and energy-efficient methods involved in thin films deposition such as chemical bath deposition and electro-deposition [11,12], (3) PbS is very sensitive to grain size (much more than in classic semiconductors like Si), which makes it a good candidate for nanostructured devices [12], and finally (4) the effect of multiple exciton generation was recently discovered in nanostructures of PbS and similar semiconductor PbSe [13], which is very promising for solar cell applications.

The theoretical studies on this type of solar cell are very rare. The first principle theoretical study of thin film solar cells with structure glass/ITO/CdS/PbS/Al was presented in Ref. [14], where the maximum cell efficiency of 4.13% was obtained at absorber thickness of 2 μm which is considered greater than those obtained experimentally.

The current study aims at enhancing the performance of the thin film CdS/PbS photovoltaic solar cells through studying some effective parameters of transparent conducting oxide (TCO) layer indium tin oxide (ITO), window layer (CdS), absorber layer (PbS) and back contact layer. The dependence of spectral quantum efficiency, short-circuit current density, fill factor, open-circuit voltage and the efficiency of CdS/PbS thin film solar cells on the thickness of ITO, thickness of CdS, minority carrier lifetime and reflectivity from back contact under illumination condition of AM 1.5 will be considered in this work. In our previous work [14], the lifetime of electron (minority carrier in PbS layer) was assumed to be 10^{-9} s. According to Graham et al. [15], the electron lifetime was assumed to be several microseconds. Therefore, in this study the lifetime has been assumed to be in the range of 10^{-10} to 10^{-6} s. The calculations carried out are based on the reflection losses from different layers, absorption losses in front-contact and window layers, front recombination, back recombination of absorber layer and recombination in space-charge region.

2. Theoretical concepts

The typical CdS/PbS device is a p–n heterojunction photodiode. CdS/PbS solar cells employ a highly transparent glass to achieve high efficiencies. The glass is sequentially coated with a TCO layer such as ITO, CdS as a window layer (used as *n*-type), PbS as an absorber layer (used as *p*-type) and is then covered with a back contact.

2.1. *Optical losses in thin-film solar cells*

For sure, a certain part of the incident solar radiation will be lost when it passes through the glass plate, TCO layer and window layer before racing the photoelectricity active absorber layer. These losses are resulting from reflection between two neighbouring media as well as absorption within TCO and CdS layers.

Accounting for multiple reflections within different layers of CdS/PbS solar cells, the total transmittance for L layers can be expressed as [16,17]:

$$T_R = 4\frac{n_1 n_2}{(n_1+n_2)^2}\prod_{j=2}^{L-1}\frac{4\frac{n_j n_{j+1}}{(n_j+n_{j+1})^2}}{\left(1-\frac{(n_j-n_{j-1})^2(n_j-n_{j+1})^2}{(n_j+n_{j-1})^2(n_j+n_{j+1})^2}\right)} \tag{1}$$

where n_1, n_2, … n_{L-1} are the refractive index of air, glass,… and PbS layer, respectively.

When the absorption effect in both ITO and CdS layers takes place, the transmission spectrum can be written as:

$$T(\lambda) = T_R\,(e^{-\alpha_1 d_1})(e^{-\alpha_2 d_2}) \tag{2}$$

where α_1, α_2, d_1, d_2 are the absorption coefficients and thicknesses of ITO and CdS layers, respectively. The absorption coefficient is calculated from:

$$\alpha(\lambda) = \frac{4\pi}{\lambda}k \tag{3}$$

where k is the extinction coefficient of the used material. According to Equation 2, the ratio of the transmitted light that reaches the absorber layer can be computed and hence the ratio of reflection and absorption losses (optical losses) can be determined. This means that a part of the incident energy which can be converted into a usable energy by the solar cell is lost by reflection and absorption.

2.2. *Quantum efficiency of thin-film solar cells*

Quantum efficiency is defined as the ratio of electrical charges extracted from a solar cell to the number of incident photons. In the following, we distinguish between the external quantum efficiency (η_{ex}) and the internal quantum efficiency (η_{in}). The exact solution of the continuity equation for the space-charge region and the neutral part of the absorber layer with taking into account the drift and diffusion components and recombination at the front surface and back surface has been found in some previous work [18–22]. Quantum efficiency of a solar cell always includes the drift and diffusion components, which are obliged to photogeneration of electron–hole pairs in the space-charge region (SCR) and in the neutral part (s) of the diode structure, respectively.

The drift component of the quantum efficiency taking into account the recombination at front surface of the absorber layer is given by [18]:

$$\eta_{\text{drift}} = \frac{1+\frac{S}{D_n}\left(\alpha+\frac{2}{W}\frac{\varphi_0-qv}{kT}\right)^{-1}}{1+\frac{S}{D_n}\left(\frac{2}{W}\frac{\varphi_o-qv}{kT}\right)^{-1}} - \exp(-\alpha W) \tag{4}$$

where S is the front surface recombination velocity; v is the applied voltage; φ_o is the barrier height; D_n is the diffusion coefficient of electrons related to their mobility μ_n by the Einstein relation $qD_n/kT = \mu_n$; W is the width of the space-charge region; α is the absorption coefficient of PbS at a given wavelength, q is the electron charge, k is the Boltzmann constant and T is room temperate.

The diffusion component of the quantum efficiency taking into account the recombination at back surface of the absorber layer is given by [19]:

$$\eta_{\text{dif}} = \frac{\alpha L_n}{\alpha^2 L_n^2 - 1} \exp(-\alpha W) \times \left\{ \alpha L_n - \frac{\frac{S_b L_n}{D_n}\left[\cosh\left(\frac{d-W}{L_n}\right) - \exp(-\alpha(d-W))\right] + \sinh\left(\frac{d-W}{L_n}\right) + \alpha L_n \exp(-\alpha(d-W))}{\frac{S_b L_n}{D_n}\sinh\left(\frac{d-W}{L_n}\right) + \cosh\left(\frac{d-W}{L_n}\right)} \right\} \quad (5)$$

where $L_n = (\tau_n D_n)^{1/2}$ is the electron diffusion length; τ_n is the electron lifetime; S_b is the velocity of recombination at the rear surface of the absorber layer and d is its thickness.

It is clear that both the components of the internal quantum efficiency are dependent on the width of SCR which can be given by [19]:

$$W = \sqrt{\frac{2\varepsilon\varepsilon_0(\varphi_0 - qv)}{q^2(N_a - N_d)}} \quad (6)$$

where ε is the relative permittivity of the semiconductor, ε_0 is the permittivity of free space and $(N_a - N_d)$ is the concentration of uncompensated acceptors.

The sum of Equations (4) and (5) gives the expression of the internal quantum efficiency (η_{int}).

Taking into account the optical losses of the incident solar radiation and using the Equations (2), (4), and (5), the external spectral quantum efficiency η_{ex} can be written in the form:

$$\eta_{\text{ex}} = T(\lambda)(\eta_{\text{drift}} + \eta_{\text{dif}}) \quad (7)$$

If the value of quantum efficiency is less than unity, this means that a part of generated electron–hole pairs is not collected by the solar cell and in this case we can determine the recombination losses at front and back surface of the absorber layer. Moreover, there is a probability that the generated electron–hole pair to recombine within the SCR and make losses of the photocurrent in the circuit of photovoltaic device. These losses are dependent on some parameters such as: carrier lifetime (τ_n, τ_p), carrier mobility (μ_n, μ_p), the width of SCR (W) and the strength of the electric-field (F).

The mean distance (the electron drift length) that the electron travels during the mean lifetime τ_n along the electric field is determined by the electron mobility μ_n and the electric field strength F:

$$\lambda_n = \mu_n F \tau_n \quad (8)$$

Then, the hole drift length is given by:

$$\lambda_p = \mu_p F \tau_p \quad (9)$$

In the Schottky diode, an electric field is not uniform, but consideration of non-uniformity is simplified, since the field strength decreases linearly with x coordinate.

In this case, the field strength F in the expressions (8) and (9) for λ_n and λ_p can be replaced by the average values of F in the sections (0, x) and (x, W) for electrons and holes, respectively [23]:

$$F(0,x) = \frac{\Phi_0 - ev}{eW}\left(2 - \frac{x}{W}\right) \tag{10}$$

$$F(x,W) = \frac{\Phi_0 - ev}{eW}\left(1 - \frac{x}{W}\right) \tag{11}$$

The charge collection efficiency is expressed by the known Hecht equation [24]:

$$\eta_c = \frac{\mu_p F(x,W)\tau_p}{W}\left[1 - \exp\left(-\frac{W-x}{\mu_p F(x,W)\tau_p}\right)\right] + \frac{\mu_n F(0,x)\tau_n}{W}\left[1 - \exp\left(-\frac{x}{\mu_n F(0,x)\tau_n}\right)\right] \tag{12}$$

The key parameter in these equations of quantum efficiency is the carrier lifetime, therefore the current study will be carried out based on the lifetime of minority carriers (electrons) in PbS layer.

2.3. *Effect of back contact*

Development of a stable and efficient back contact is essential for the long term stability of thin film solar cells. In order to get good Ohmic contact between the absorber layer and metal back electrode, a semiconductor thin film is usually introduced to lower the mismatch of the work-function between the absorber and the metal electrode [25]. Paudel et al. [26] used the following formula to assess theoretically the effect of the reflection from back contact on the internal (or external) quantum efficiency and hence on the short-current density.

$$\eta_{\text{int}}(R) = \eta_{\text{int}}[1 + R \times \exp(-\alpha d)] \tag{13}$$

where R is the reflectivity from the back contact, α is the absorption coefficient of the absorber layer and d is its thickness.

2.4. *Short-circuit current density of thin-film solar cells*

The optical and recombination losses can be estimated quantitatively by calculating the short-circuit current density (J_{SC}). In general, J_{SC} is described by the following expression:

$$J_{\text{SC}} = q \sum_i T(\lambda)\,\frac{\phi_i(\lambda_i)}{hv_i}\eta_{\text{int}}(\lambda_i)\Delta\lambda_i \tag{14}$$

where ϕ_i is the spectral power density, hv is the photon energy, $\Delta\lambda_i$ is the interval between the two neighbouring values λ.

2.5. *Current–voltage characteristic under illumination*

The measured *I–V* characteristics of CdS/PbS heterostructure are governed by the generation–recombination Sah–Noyce–Shockley theory [27,28]. The Sah–Noyce–Shockley theory supposes that the generation–recombination rate in the section x of the space-charge region is determined by the expression:

$$U(x,V) = \frac{n(x,V)P(x,V) - n_i^2}{\tau_p[n(x,V) + n_1] + \tau_n[P(x,V) + P_1]} \tag{15}$$

where n_i is the intrinsic carrier concentration and the values n_1 and P_1 are determined by the energy spacing between the top of the valence band and the generation–recombination level E_t, i.e.

$$P_1 = N_v \exp(-(E_t/kT) \tag{16}$$

$$n_1 = N_c \exp(-(E_g - E_t)/kT) \tag{17}$$

where E_g is the energy gap and N_c, N_v is the effective state densities in the conduction and valence bands, respectively, and given by:

$$N_c = 2\left(\frac{m_n\, KT}{h^2}\right)^{3/2}, \quad N_v = 2\left(\frac{m_p\, KT}{h^2}\right)^{3/2} \tag{18}$$

In this equation, m_n and m_p are the effective masses of electrons and holes, respectively.

The values $n(x, V)$ and $P(x, V)$ in Equation (15) are the carrier concentration in the conduction and valence bands and given by [28].

$$P(x,V) = N_c \exp\left[-\frac{\Delta\mu + \varphi(x,V)}{kT}\right] \tag{19}$$

$$n(x,V) = N_v \exp\left[-\frac{E_g - \Delta\mu - \varphi(x,V) - qV}{kT}\right] \tag{20}$$

where $\Delta\mu$ is the energy spacing between the Fermi level and the top of the valence band of PbS and $\varphi(x, V)$ is the electron energy in the space-charge region is given by:

$$\varphi(x,V) = (\varphi_0 - qV)\left(1 - \frac{x}{W}\right) \tag{21}$$

According to the Equations (15)–(21), the recombination–generation current is found by the integration of $U(x, V)$ throughout the entire depletion layer [18]:

$$J_{\mathrm{gr}} = q\int_0^W U(x,V)\,dx \tag{22}$$

In addition to the recombination–generation current, there is another current contributing to the dark current which is called the over-barrier current density J_n and can be written in the form [29]:

$$J_n = = q\frac{n_p L_n}{\tau_n}\left[\exp\left(\frac{qV}{kT}\right) - 1\right] \tag{23}$$

where n_p is the concentration of electrons in the bulk part of the p-type layer (PbS), given by:

$$n_p = N_c \exp\left(-\frac{E_g - \Delta\mu}{kT}\right) \tag{24}$$

Thus, the dark current density in CdS/PbS heterostructure $J_d(V)$ is the sum of the generation–recombination and over-barrier components:

$$J_d(V) = J_{\mathrm{gr}}(V) + J_n(V) \tag{25}$$

Thus, the illuminated J–V characteristic can be presented in the form:

$$J(V) = J_d - J_{\mathrm{ph}} \tag{26}$$

where J_{ph} is the photocurrent density.

The values of all parameters used in this work are listed in Table 1.

3. Results and discussion

The transmission spectrum of the glass/ ITO/CdS structure is calculated using Equation (2) and plotted in Figure 1 at different thicknesses of ITO (d_{ITO}) and CdS (d_{CdS}) layers. The calculations are based on the optical constants (refractive index n and extinction coefficient k of the used materials) which are taken from Ref. [33]. The refractive index of glass plate is calculated using Sellmeier dispersion equation [34] and its extinction coefficient is assumed to be equal to zero. The calculations are carried out based on some assumptions such as the refractive index, extinction coefficient and the absorption

Table 1. The values of the parameters used in this study.

Symbol	Value	References
Φ_0-qv	0.7 eV	Current work
D_n	25.8	Current work
μ_n	1000 cm^2/(V S)	Current work
S	10^7 cm/s	Current work
S_b	10^7 cm/s	Current work
d	3 μm	Current work
ϵ	18	[30]
μ_p	80 cm^2/(V S)	Current work
E_g	0.41 eV	[31]
m_n	0.085 m_e	[32]
m_p	0.085 m_e	[32]
$\Delta\mu$	0.047 eV	Current work

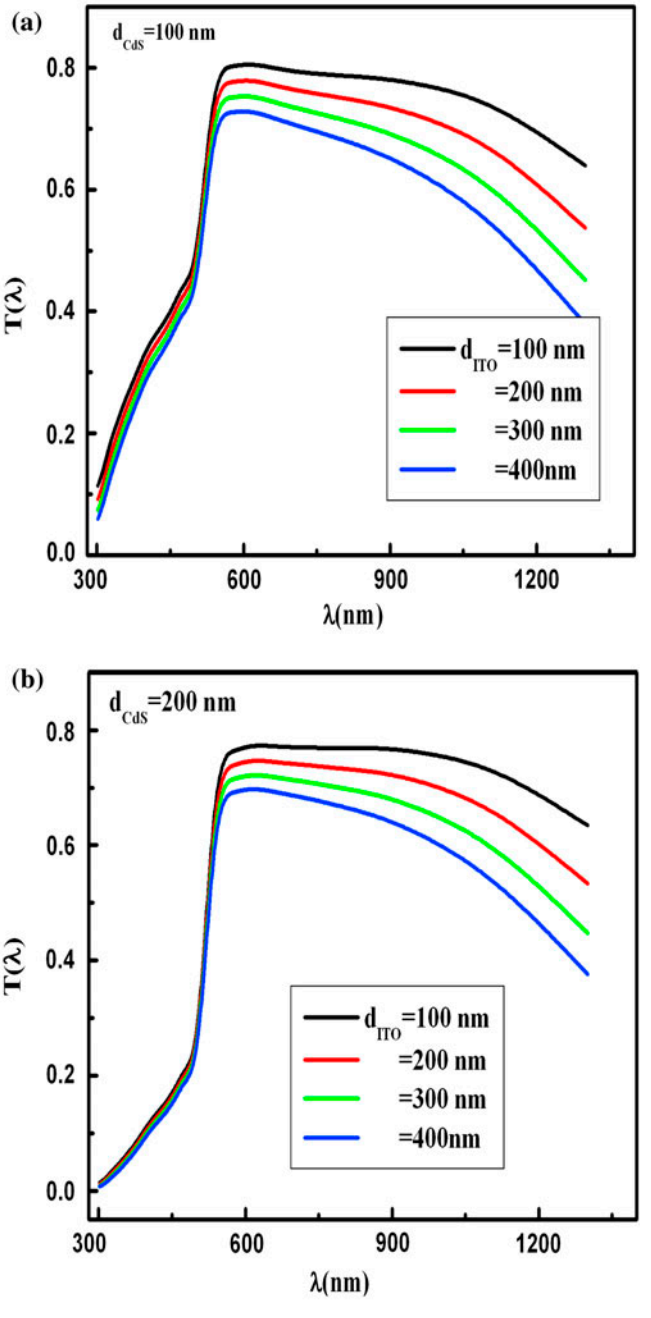

Figure 1. (colour online) Calculated transmission spectrum $T(\lambda)$ of CdS/PbS solar cell as a function of the thickness of ITO layer d_{ITO} at different thicknesses of CdS layer d_{CdS} of 100 nm (a) and 200 nm (b).

coefficient of the used materials are constants and do not change with the variation of the thickness of ITO or CdS layers. On the other hand, each layer of the solar cell was selected to satisfy some specific properties as reported in Ref. [14].

As can be seen from Figure 1(a), the transmission spectrum decreases by increasing the thickness of ITO layer. When the thickness of window layer is increased from 100 to 200 nm as shown in Figure 1(b), a further decrease in transmission is observed. The average transmission in the wavelength range of 500–850 nm is about 0.8 in the case of $d_{ITO} = 100$ nm and $d_{CdS} = 100$ nm, which means the losses caused by reflection and absorption (optical losses) are about 20%, while the average transmission of 0.68 is observed at $d_{ITO} = 400$ nm and $d_{CdS} = 200$ nm at the same range of wavelength. Thus, by thinning both the transparent conductive layer (ITO) from 400 to 100 nm and window layer (CdS) from 200 to100 nm it is possible to reduce the optical losses from 32 to 20%.

The internal quantum efficiency η_{int} is calculated using Equations (4) and (5) and the results are plotted in Figure 2 as a function of electron lifetime τ_n at different values of $N_a - N_d$. As shown in Figure 2(a), when the space-charge region is wide ($N_a - N_d$ is small) the effect of electron lifetime on the internal quantum efficiency can be neglected. The internal quantum efficiency decreases by decreasing both the electron lifetime and the width of space-charge region (increasing $N_a - N_d$) as shown in Figure 1(b) and (c). The decrease in internal quantum efficiency with the increase in $N_a - N_d$ can be attributed to the larger portion of photons which are absorbed outside the space-charge region [23]. The decrease in internal quantum efficiency with the decrease in the electron lifetime is due to the fact that recombination losses become more effective at low values of lifetime. The same behaviour is observed for the dependence of external quantum efficiency η_{ex} on τ_n and $N_a - N_d$ as shown in Figure 3. As expected, the values of calculated η_{ex} are smaller than the values of η_{in} due to the reflection losses from different layers in CdS/PbS cell as well as the absorption losses in ITO and CdS layers.

Figure 4 represents the dependence of spectral internal and external quantum efficiency on the ratio of reflectivity from metallic back contact. The obtained results are carried out at $\tau_n = 10^{-6}$ s and $N_a - N_d = 10^{16}$ cm^{-3}. As shown in this figure, both the internal quantum efficiency and external quantum efficiency are increased by increasing the ratio of reflectivity from the metallic back contact. This result implies a significant effect of the back contact layer on the quantum efficiency and hence on the short-circuit current density.

Figure 5 shows the charge collection efficiency (η_c) computed by Equation (12) for different lifetimes and at fixed concentration of uncompensated acceptors ($N_a - N_d$) of 10^{15} cm^{-3}. It is clear that η_c increases by increasing the value of x (which is measured from PbS side) and attains to saturation case when x is close to the width of space-charge region (W). Moreover, η_c increases by increasing the electron lifetime and its value is close to unity at $\tau_n = 10^{-6}$ s. This indicates, the recombination losses in space-charge region can be ignored at high values of electron lifetime and this process has a considerable effect at low lifetime. The losses due to recombination are about 80% at $x = 0$, $\tau_n = 10^{-10}$ s and much less losses (13%) are observed at $x = W$ at $\tau_n = 10^{-10}$ s.

The drift component of the short-circuit current density J_{drift} is calculated from Equation (14) using the drift component of the internal quantum efficiency (Equation (4)). It is clear from Equation (4) that the drift component of internal quantum

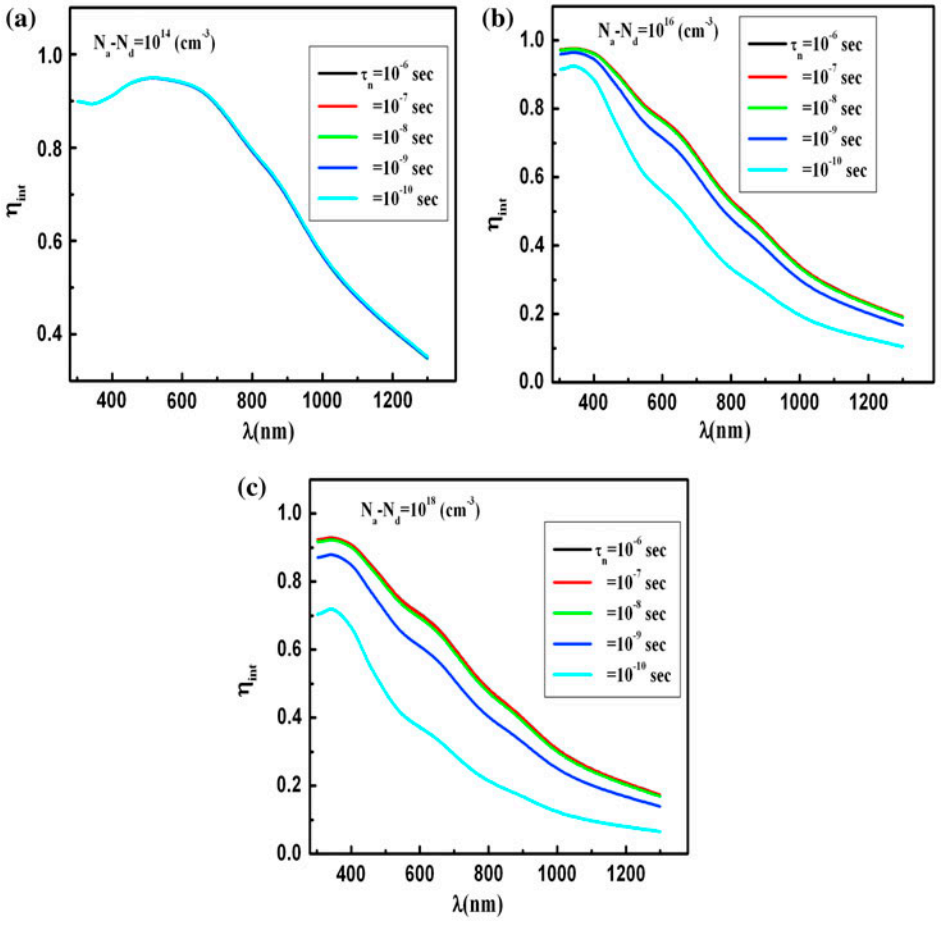

Figure 2. (colour online) Internal spectral quantum efficiency η_{int} as a function of electron lifetime τ_n at different values of concentration of uncompensated acceptors of $N_a - N_d = 10^{14}$ cm^{-3} (a), $N_a - N_d = 10^{16}$ cm^{-3} (b) and $N_a - N_d = 10^{18}$ cm^{-3} (c).

efficiency is mainly dependent on the width of space-charge region (W). Therefore, the dependence of J_{drift} on $N_a - N_d$ (or in W) is shown in Figure 6(a). It is clear that J_{drift} decreases by increasing $N_a - N_d$ (decreasing W). It is known that by increasing $N_a - N_d$, the electric field becomes stronger and consequently the surface recombination becomes weaker resulting in an increase in J_{drift}. However in current work, J_{drift} decreases with $N_a - N_d$ because a significant portion of the radiation is absorbed outside the space-charge region as shown in Figure 2. This behaviour is observed by Kosyachenko et al. in their study of CdS/CdTe solar cell [18]. On the other hand, Figure 6(b) represents the dependence of diffusion component of the short-circuit current density J_{dif} on electron lifetime τ_n at various values of $N_a - N_d$. It can be seen that J_{dif} increases by increasing $N_a - N_d$ and τ_n. The maximum value of J_{dif} is about 14 mA/cm^2 at $\tau_n = 10^{-6}$

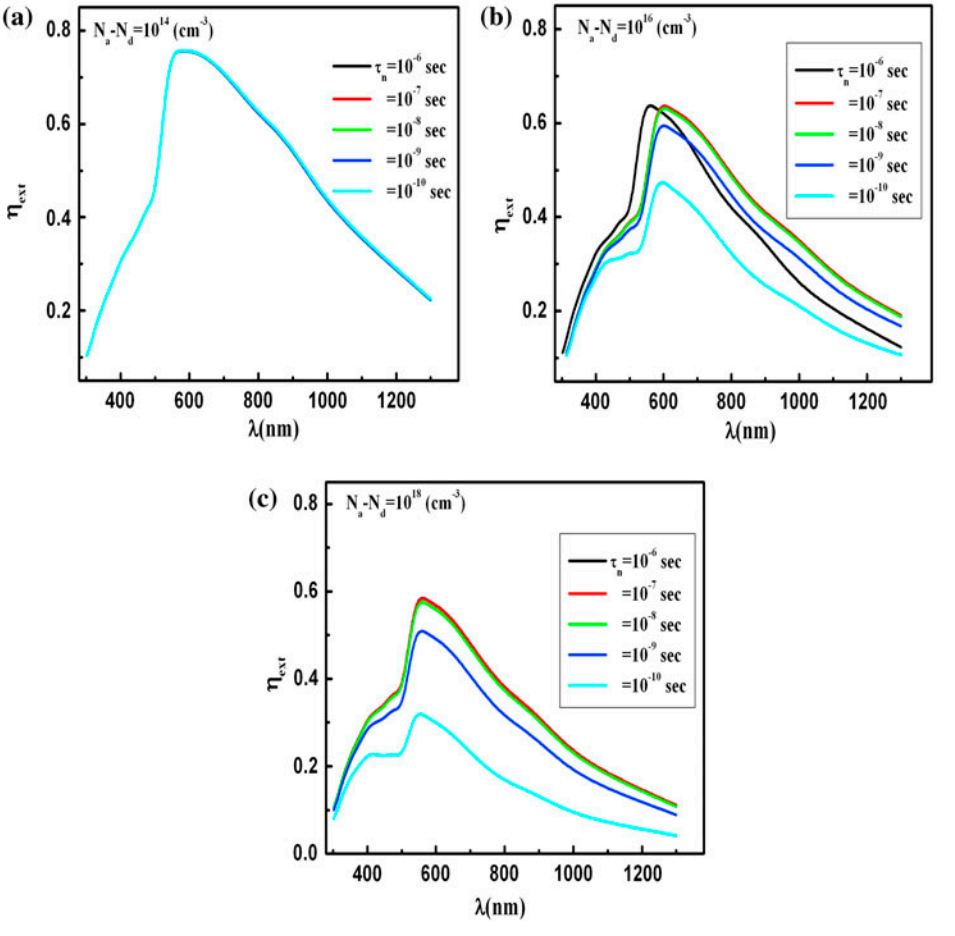

Figure 3. (colour online) External spectral quantum efficiency η_{ex} as a function of electron lifetime τ_n at different values of concentration of uncompensated acceptors of $N_a - N_d = 10^{14}$ cm^{-3} (a), $N_a - N_d = 10^{16}$ cm^{-3} (b) and $N_a - N_d = 10^{18}$ cm^{-3} (c).

s and $N_a - N_d = 10^{18}$ cm^{-3}. Also this figure that refers to J_{dif} is approximately constant at lifetime longer than 10^{-8} s. It can be concluded that the back surface recombination has significant effect at short lifetime and wide space-charge region.

Using the drift and diffusion components of the short-circuit current density, the total short-circuit current density J_{SC} as a function of $N_a - N_d$ at different electron lifetimes is calculated and plotted in Figure 7(a). As seen in this figure, J_{SC} decreases by increasing $N_a - N_d$. Observing the variation of J_{drift} and J_{dif} with $N_a - N_d$ as shown in Figure 6, it can be concluded that the drift component of short-circuit current density plays a significant role in the behaviour of the dependence of short-circuit current density on $N_a - N_d$. The maximum current density of 18.4 mA/cm^2 is achieved at widen space-charge region ($N_a - N_d = 10^{15}$ cm^{-3}) and the longest lifetime ($\tau_n = 10^{-6}$ s). In this case, the optical and recombination losses are about 55%. These losses increase up to 82% at $\tau_n = 10^{-10}$ s and

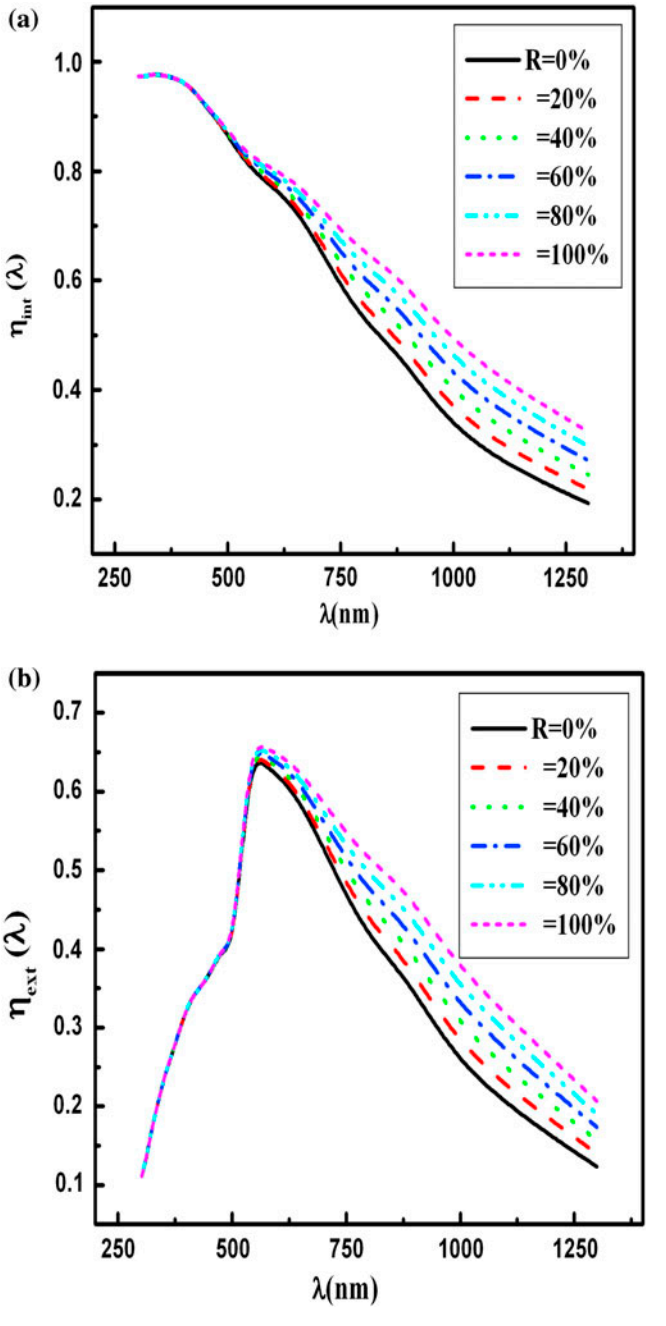

Figure 4. (colour online) Internal spectral quantum efficiency η_{int} (a) and external spectral quantum efficiency η_{ex} (b) at different ratios of reflectivity (R%) from the back contact at $\tau_n = 10^{-6}$ s and $N_a - N_d = 10^{16}$ cm^{-3}.

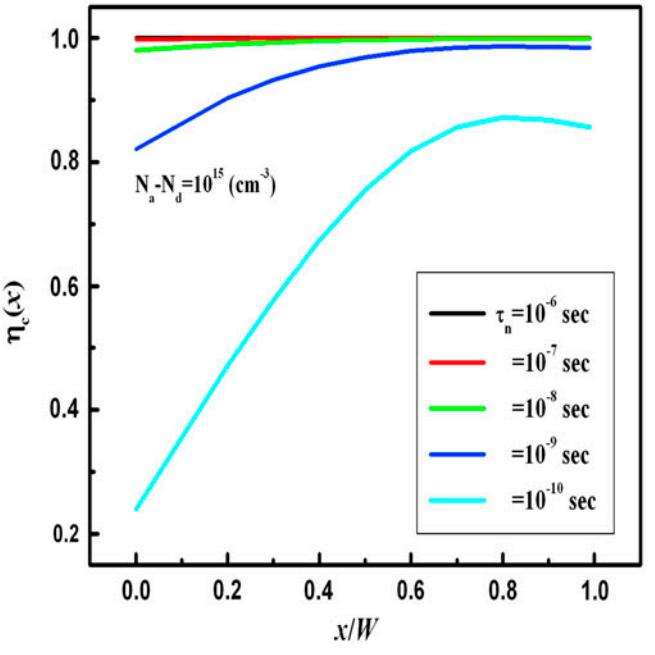

Figure 5. (colour online) The coordinate dependences of the charge-collection efficiency η_c calculated for concentration of uncompensated acceptors of $N_a - N_d = 10^{15}$ cm^{-3} and different electron lifetimes τ_n.

$N_a - N_d = 10^{18}$ cm^{-3} where the calculated current density equals 7.3 mA/cm^2. These results are obtained on the basis of the value of maximum short-circuit current density $J_{SC}^0 = 41$ mA/cm^2, which is calculated using Equation (14) when $T(\lambda)$=1 and $\eta_{int} = 1$. When the influence of reflectivity from metallic back contact is considered, the value of short-circuit current density increases by increasing the ratio of reflectivity as seen in Figure 7(b). These results are carried out at $N_a - N_d = 10^{16}$ cm^{-3}. When the back contact is 100% reflected the incident photons, J_{SC} increases up to 18.9 mA/cm^2 at $\tau_n = 10^{-6}$ s. It can be concluded that the totally reflected back contact will increase J_{SC} by a ratio of ~17% at all values of electron lifetime.

Under the illumination condition of AM1.5 solar irradiation, J–V curve of CdS/PbS solar cell at different electron lifetimes and $N_a - N_d = 10^{16}$ cm^{-3} is shown in Figure 8. It is clear that the J–V curves are shifted down by increasing the electron lifetime indicating an increase in the photo-generated current density.

Figure 9 shows J–V characteristic of CdS/PbS solar cells under illumination condition of AM1.5 solar irradiation at different ratios of reflectivity (R%) from the back contact at $\tau_n = 10^{-6}$ s and $N_a - N_d = 10^{16}$ cm^{-3}. It can be seen that the increase in the reflectivity of back contact leads to more shift-down of all curves.

The values of CdS/PbS cell efficiency (η), open-circuit voltage (V_0) and fill factor (FF) are estimated from Figure 8 and plotted in Figure 10 as a function of electron lifetime. Using the maximum current (J_m) and maximum voltage (V_m), the fill factor (FF) can be calculated from $FF = V_m J_m / J_{SC} V_0$. Besides, the cell efficiency is calculated using

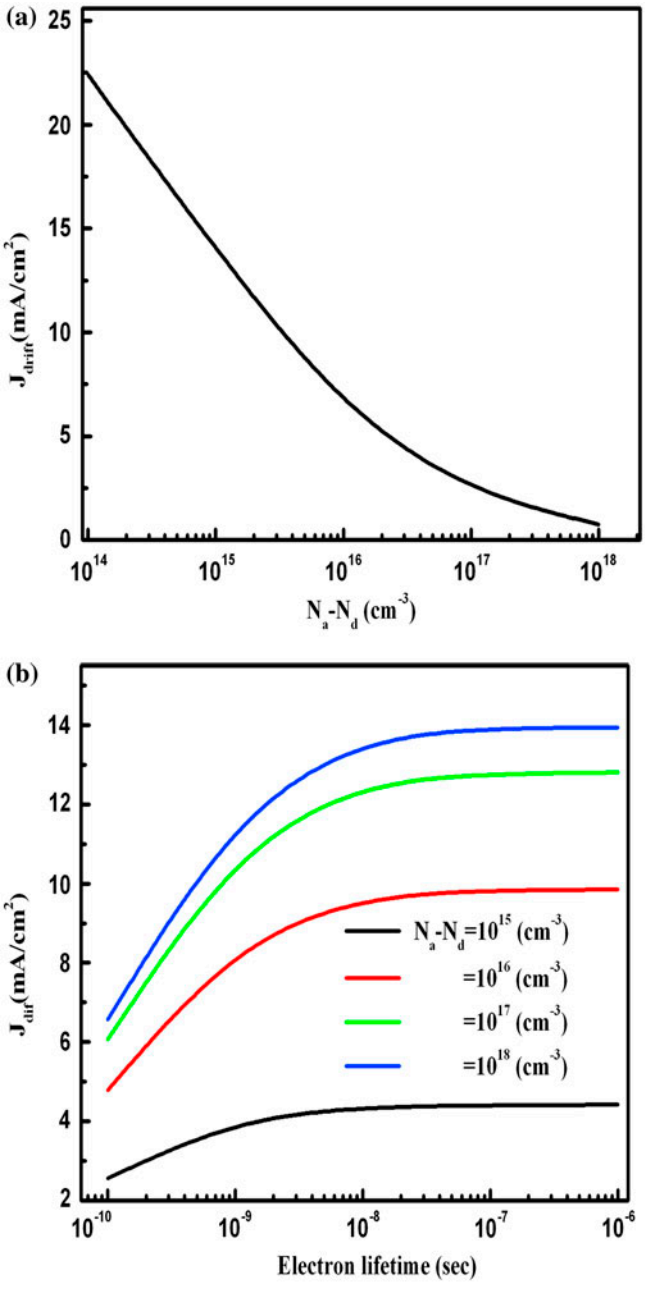

Figure 6. (colour online) Dependence of drift component J_{drift} of current density on concentration of uncompensated acceptors $N_a - N_d$ (a) and dependence of diffusion component J_{dif} of current density on electron lifetime at different concentrations of uncompensated acceptors (b).

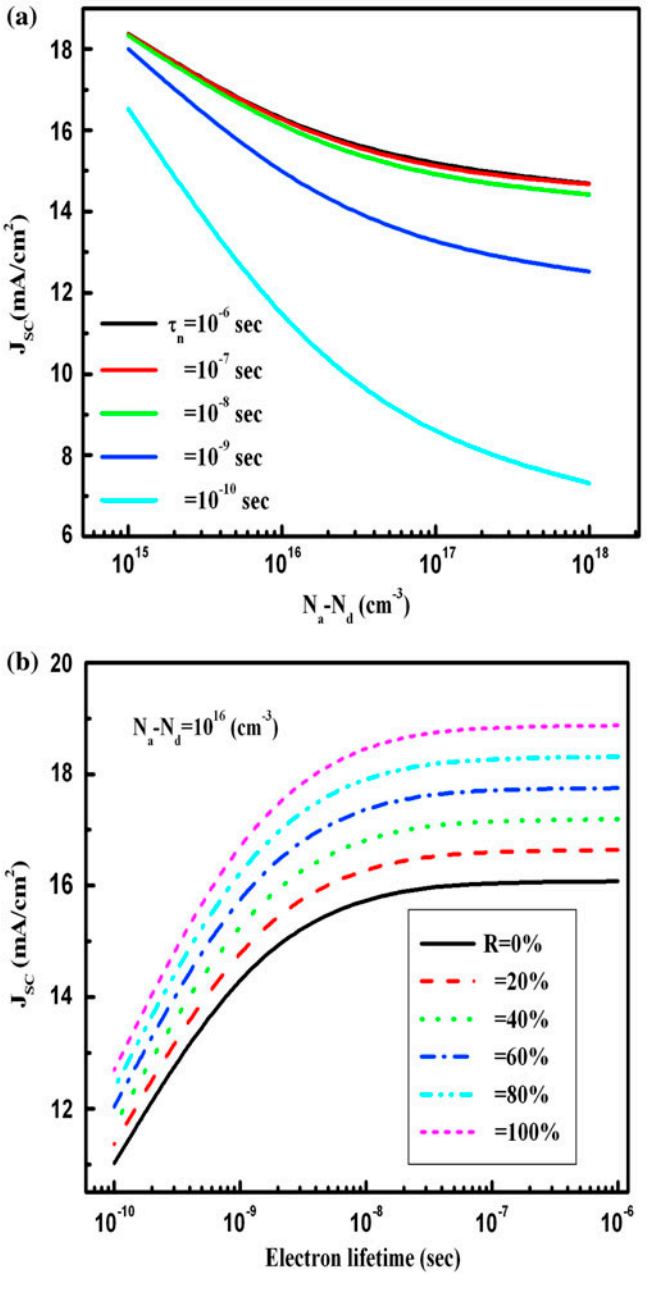

Figure 7. (colour online) Calculated short-circuit current density J_{SC} as a function of concentration of uncompensated acceptors of $N_a - N_d$ for different electron lifetimes τ_n (a) and J_{SC} at different ratios of reflectivity (R%) from the back contact at $N_a - N_d = 10^{16}$ cm^{-3}.

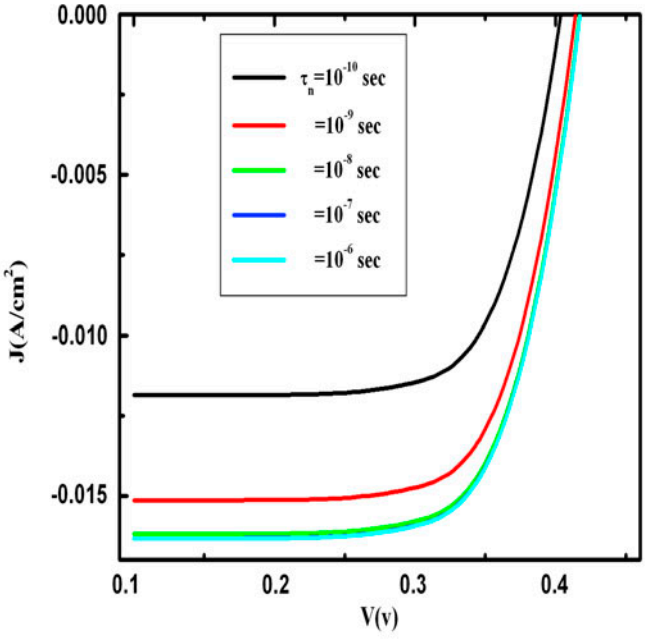

Figure 8. (colour online) *J–V* characteristic of CdS/PbS solar cells at different values of electron lifetime under illumination condition of AM1.5 solar irradiation.

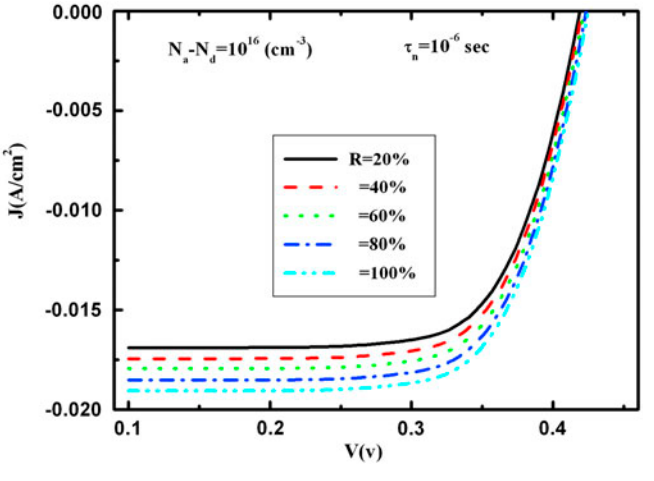

Figure 9. (colour online) *J–V* characteristic of CdS/PbS solar cells under illumination condition of AM1.5 solar irradiation at different ratios of reflectivity (*R*%) from the back contact at $\tau_n = 10^{-6}$ s and $N_a - N_d = 10^{16}$ cm^{-3}.

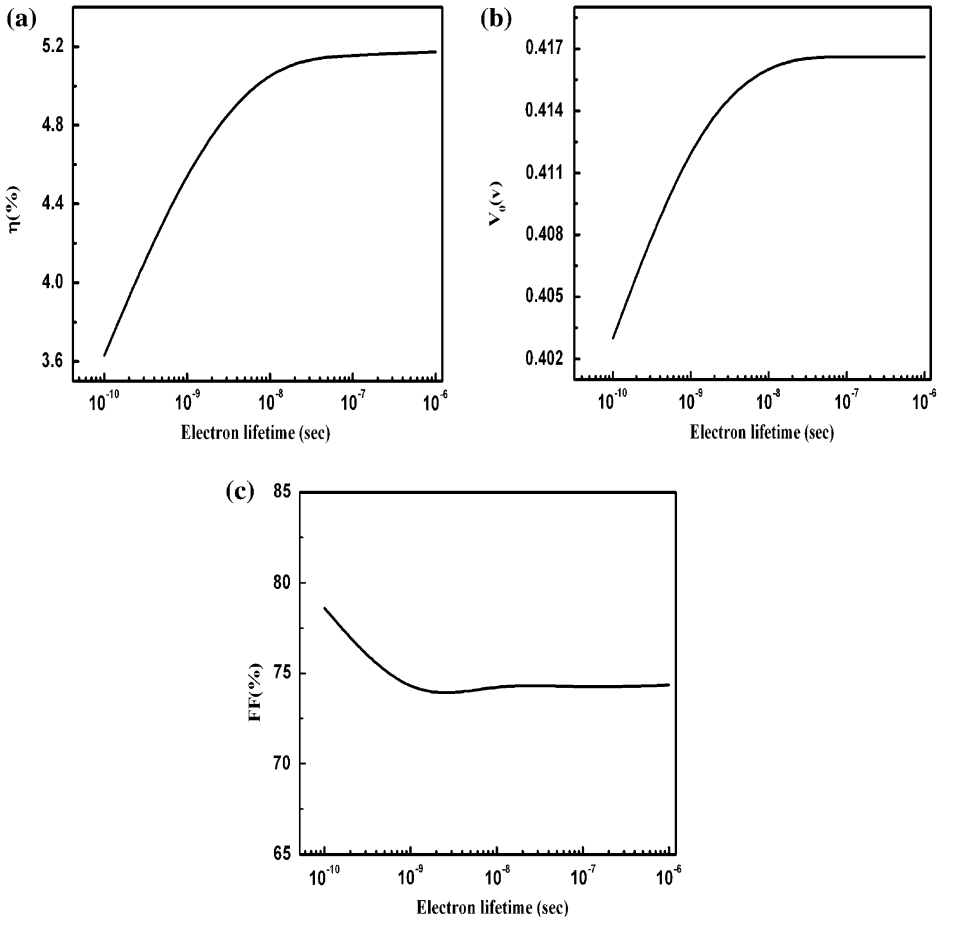

Figure 10. Dependence of the efficiency η(%) (a), open-circuit voltage V_0 (b) and fill factor FF (%) (c) on electron lifetime of CdS/PbS solar cells.

this relation $\eta = V_m J_m / P_{in}$, where P_{in} is the density of the total AM 1.5 solar radiation power (equals 96.3 mW/cm^2 [35]). Figure 10(a) shows that the efficiency is increased by increasing the lifetime and the maximum efficiency of 5.17% is achieved at $\tau_n = 10^{-6}$ s. From Figure 10(b), we can notice that the minimum value of open-circuit voltage of 402 mV is observed at shorter lifetime (10^{-10} s). With further increase in carrier lifetime up to 10^{-8} s the value of V_0 increases up to 417 mV. Finally, V_0 approaches the saturation case at the lifetime range of 10^{-8}–10^{-6} s. This saturation maybe due to the rate of generation of carriers equals the rate of its recombination, and this process limits the maximum attainable open-circuit voltage. Apart from $\tau_n = 10^{-10}$ s, the fill factor (FF) seems to be constant (74%) for different values of lifetimes as shown in Figure 10(c). When the effect of back contact is taken into calculation, the maximum current density, the maximum voltage, the open-circuit voltage and the cell efficiency are estimated from Figure 9 and listed in Table 2. It is clear that all these parameters increase by increasing the ratio of reflectivity. The maximum efficiency of 6.1% is

Table 2. The maximum current density (J_m), maximum voltage (V_m), open-circuit voltage (V_0) and efficiency (η) of thin film CdS/PbS solar cells at different ratios of reflectivity from back contact at $\tau_n = 10^{-6}$ s and $N_a - N_d = 10^{16}$ cm^{-3}.

R(%)	V_0 (V)	V_m (V)	J_m (mA/cm^2)	η (100)
20	0.418	0.334	15.62	5.42
40	0.419	0.338	15.82	5.55
60	0.420	0.342	16.16	5.74
80	0.424	0.343	16.73	5.95
100	0.425	0.346	16.91	6.08

achieved at $\tau_n = 10^{-6}$ s and $N_a - N_d = 10^{16}$ cm^{-3}. It can be concluded that as the reflectivity from back contact is 100%, it leads to an increase in the efficiency of CdS/PbS solar cell by a ratio of 18%. The values of efficiency that are estimated in this work are considered greater than the corresponding values in some other experimental studies. For example, Bhandari et al. [36] obtained efficiency of about 3.3%, Hernandez-Borja et al. [12] achieved efficiency of 1.63%, and the efficiency that was reported by Obaid et al. [9, 10] is about 1.68 and 1.37%, respectively.

4. Conclusions

This work studies the influence of the thickness of ITO, CdS layer, the minority lifetime and the reflectivity of metallic back contact on the performance of thin film CdS/PbS solar cells. The maximum transmission spectrum of 0.8 is achieved at 100 nm thickness of both ITO and CdS layer where the optical losses are about 20%. The effect of electron lifetime (τ_n) on the external and internal quantum efficiency can be neglected at low concentration of uncompensated acceptors $N_a - N_d$ (wide space-charge region). The values of external and internal quantum efficiency decrease by decreasing the lifetime at small width space-charge region due to the recombination losses, which become more effective at low values of lifetime. The recombination losses in space-charge region can be ignored at high values of electron lifetime and these losses reach 25% at the half width of space-charge region at lifetime of 10^{-10} s. The J–V curves are shifted down by increasing the electron lifetime and the ratio of reflectivity from back contact indicating an increase in the photo-generated current density under the illumination condition of AM1.5 solar irradiation. The maximum efficiency of 5.17%, maximum open-circuit voltage of 417 mV and fill factor of 74% are performed at $d_{ITO} = 100$ nm, $d_{CdS} = 100$ nm, $\tau_n = 10^{-6}$ s and $N_a - N_d = 10^{16}$ cm^{-3}. When the effect of back contact is considered, the values of these parameters are increased by increasing the ratio of reflectivity, and the efficiency records a value of 6.1% when the back contact is totally reflected.

Acknowledgement

The author would like to thank the Deanship of Scientific Research, King Saud University, Riyadh, Saudi Arabia, for funding and supporting this research.

References

[1] T.M. Razikov, C.S. Ferekides, D. Morel, E. Stefanakos, H.S. Ullal and H.M. Upadhyaya, Solar Energy 85 (2011) p.1580.
[2] A. Goetzberger and C. Hebling, Sol. Energy Mater. Sol. Cells 62 (2000) p.1.
[3] A. Goodrich and M. Woodhouse, *PV Manufacturing Cost Analysis: Future Cost Reduction Opportunities*, National Renewable Energy Laboratory (NREL), Golden, CO, 2012.
[4] W.U. Huynh, J.J. Dittmer and A.P. Alivisatos, Science 295 (2002) p.2425.
[5] M.A. Green, K. Emery, Y. Hishikawa, W. Warta and E.D. Dunlop, Prog. Photovoltaics Res. Appl. 21 (2013) p.1.
[6] J.H. Borja, Y.V. Vorobiev and R.R. Bon, Sol. Energy Mater. Sol. Cells 95 (2011) p.1882.
[7] N.R. Mathews, C.A. Chavez, M.A.C. Jacome and J.A.T. Antonio, Electrochim. Acta 99 (2013) p.76.
[8] H. Moreno-Garcia, M.T.S. Nair and P.K. Nair, Thin Solid Films 519 (2011) p.2287.
[9] A.S. Obaid, M.A. Mahdi, Z. Hassan and M. Bououdina, Superlattices Microstruct. 52 (2012) p.816.
[10] A.S. Obaid, M.A. Mahdi, Z. Hassan and M. Bououdina, Int. J. Hydrogen Energy 38 (2013) p.807.
[11] M.G. Sandoval-Paz and R. Ramırez-Bon, Thin Solid Films 517 (2009) p.6747.
[12] J. Hernandez-Borja, Y.V. Vorobiev and R. Ramırez-Bon, Sol. Energy Mater. Sol. Cells 95 (2011) p.1882.
[13] R.J. Ellingson, M.C. Beard, J.C. Johnson, P. Yu, O.I. Micic, A.J. Nozik, A. Shabaev and A.L. Efros, Nano Lett. 5 (2005) p.865.
[14] H.A. Mohamed, Sol Energy, 108 (2014) p.360.
[15] R. Graham, C. Miller, E. Oh and D. Yu, Nano Lett. 11 (2011) p.717.
[16] F.W. Mont, J.K. Kim, M.F. Schubert, H. Luo, E.F. Schubert and R.W. Siegel, Proc. SPIE 6486 (2007) p.64861C.
[17] F.W. Mont, J.K. Kim, M.F. Schubert, E.F. Schubert and R.W. Siegel, J. Appl. Phys. 103 (2008) p.083120.
[18] L.A. Kosyachenko, A.I. Savchuk and E.V. Grushko, Thin Solid Films 517 (2009) p.2386.
[19] V.V. Brus, Sol. Energy 86 (2012) p.786.
[20] L.A. Kosyachenko, X. Mathew, V. Ya. Roshko and E.V. Grushko, Sol. Energy Mater. Sol. Cells 114 (2013) p.179.
[21] H.A. Mohamed, Can. J. Phys. (2014) doi:10.1139/cjp-2013-0477.
[22] H.A. Mohamed, J. Optoelectron. Adv. Mater. 16 (2014) p.333.
[23] L.A. Kosyachenko, E.V. Grushko and V.V. Motushchuk, Sol. Energy Mater. Sol. Cells 90 (2006) p.2201.
[24] K. Hecht, Z. Phys. 77 (1932) p.235.
[25] L. Zhi, F. Lianghuan, Z. Guanggen, L. Wei, Z. Jingquan, W. Lili and W. Wenwu, J. Semicond. 41 (2013) p.014008.
[26] N.R. Paudel, K.A. Wieland and A.D. Compaan, Sol. Energy Mater. Sol. Cells 105 (2012) p.109.
[27] C. Sah, R. Noyce and W. Shokley, Proc. IRE 45 (1957) p.1228.
[28] L.A. Kosyachenko, V.M. Sklyarchuk, O.F. Sklyarchuk and V.A. Gnatyuk, Semicond. Sci. Technol. 22 (2007) p.911.
[29] S. Sze, *Physics of Semiconductor Devices* 2nd ed., Wiley, New York, 1981.
[30] J. Akhtar, M. Azad Malik, P. O'Brien, K.G.U. Wijayantha, R. Dharmadasa, S.J.O. Hardman, D.M. Graham, B.F. Spencer, S.K. Stubbs, W.R. Flavell, D.J. Binks, F. Sirotti, M. El Kazzi and M. Silly, J. Mater. Chem. 20 (2010) p.2336.
[31] Y. Zhang, Z. Li, J. Ouyang, S. Tsang, J. Lu, K. Yu, J. Ding and Y. Tao, Org. Electron. 13 (2012) p.2773.

[32] S. Baskoutas, A.F. Terzis and W. Schommers, J. Comput. Theor. Nanosci. 3 (2006) p.269.
[33] Available at http://homepages.rpi.edu/schubert/Educational-resources/Materials-efractive-index-and-extinction-coefficient.pdfS.
[34] S.O. Kasap, *Optoelectronics and Photonics: Principles and Practice*, Prentice-Hall, New Jersey, NJ, 2000.
[35] T. Toshifumi, S. Adachi, H. Nakanishi and K. Ohtsuka, Jpn. Appl. Phys. 32 (1993) p.3496.
[36] K.P. Bhandari, et al., Sol. Energy Mater. Sol. Cells 117 (2013) p.476.